Cell

Visualization of Eukaryotic DNA Mismatch Repair Reveals Distinct Recognition and Repair Intermediates

Hans Hombauer,[1,2,3,5] Christopher S. Campbell,[1,3,5] Catherine E. Smith,[1,2,3] Arshad Desai,[1,3] and Richard D. Kolodner[1,2,3,4,*]
[1]Ludwig Institute for Cancer Research
[2]Department of Medicine
[3]Department of Cellular and Molecular Medicine, Moores-UCSD Cancer Center
[4]Institute of Genomic Medicine
University of California School of Medicine, San Diego, 9500 Gilman Drive, La Jolla, CA 92093-0669, USA
[5]These authors contributed equally to this work
*Correspondence: rkolodner@ucsd.edu
DOI 10.1016/j.cell.2011.10.025

SUMMARY

DNA mismatch repair (MMR) increases replication fidelity by eliminating mispaired bases resulting from replication errors. In *Saccharomyces cerevisiae*, mispairs are primarily detected by the Msh2-Msh6 complex and corrected following recruitment of the Mlh1-Pms1 complex. Here, we visualized functional fluorescent versions of Msh2-Msh6 and Mlh1-Pms1 in living cells. We found that the Msh2-Msh6 complex is an S phase component of replication centers independent of mispaired bases; this localized pool accounted for 10%–15% of MMR in wild-type cells but was essential for MMR in the absence of Exo1. Unexpectedly, Mlh1-Pms1 formed nuclear foci that, although dependent on Msh2-Msh6 for formation, rarely colocalized with Msh2-Msh6 replication-associated foci. Mlh1-Pms1 foci increased when the number of mispaired bases was increased; in contrast, Msh2-Msh6 foci were unaffected. These findings suggest the presence of replication machinery-coupled and -independent pathways for mispair recognition by Msh2-Msh6, which direct formation of superstoichiometric Mlh1-Pms1 foci that represent sites of active MMR.

INTRODUCTION

DNA mismatch repair (MMR) catalyzes a postreplication excision reaction that increases the fidelity of DNA replication by eliminating mispaired bases resulting from replication errors (Iyer et al., 2006; Kolodner, 1996; Kolodner and Marsischky, 1999). MMR defects cause increased mutation rates, and in mammals this results in the development of different cancers (Peltomäki, 2003). In addition, MMR acts on mispaired bases in recombination intermediates and also prevents recombination between divergent DNA sequences, preventing genome rearrangements (Datta et al., 1996; Matic et al., 1995; Putnam et al., 2009). Mispaired bases are recognized by MutS in bacteria (Iyer et al., 2006) and by two partially redundant MutS-related heterodimer complexes, Msh2-Msh6 or Msh2-Msh3, in eukaryotes (Marsischky et al., 1996). Msh2-Msh6 is more abundant than Msh2-Msh3 (Genschel et al., 1998; Ghaemmaghami et al., 2003) and likely promotes most MMR in eukaryotes. Msh2-Msh3 primarily corrects mispairs that are not efficiently repaired by Msh2-Msh6 and acts when Msh2-Msh6 is absent due to loss of Msh6 (Genschel et al., 1998; Marsischky et al., 1996; Sia et al., 1997). After the mismatch recognition factors bind a mispaired base, accessory factors including MutL in bacteria and the Mlh1-Pms1 (*S. cerevisiae* Pms1 = human Pms2) or Mlh1-Mlh3 complexes in eukaryotes are recruited, targeting repair to the daughter DNA strand (Cannavo et al., 2005; Flores-Rozas and Kolodner, 1998; Iyer et al., 2006; Kunkel and Erie, 2005; Prolla et al., 1994).

Recent studies in *S. cerevisiae* using next-generation sequencing to detect mutations in an MMR-defective *mlh1* mutant indicate that the rate of accumulating mispair bases, including both base:base and frameshift mispairs in repeat sequences, is approximately 0.1 mispaired base per cell division (Zanders et al., 2010). This rate is consistent with the rate of accumulation of nucleotide changes in *URA3* and *CAN1* (Lang and Murray, 2008) in wild-type *S. cerevisiae* multiplied by the known increase in mutation rate at these genes in MMR-defective mutants. Thus, it appears that MMR must be able to recognize 1 mispaired base per genome (~12,000,000 base pairs). Remarkably, in vitro, mismatch recognition proteins exhibit only modestly higher affinity for mispaired DNA than for DNA containing only base pairs ranging from 3- to 20-fold (Alani, 1996; Iaccarino et al., 1998; Jiricny et al., 1988; Marsischky and Kolodner, 1999) to recently reported 60- to 400-fold affinity differences depending on the specific mispair (Huang and Crothers, 2008). Mispair binding licenses an ATP-binding-induced conversion of MutS, Msh2-Msh6, and Msh2-Msh3 to

a sliding clamp form trapped on DNA; in the absence of mispairs, ATP induces direct dissociation of these proteins from DNA (Acharya et al., 2003; Gradia et al., 1999; Mendillo et al., 2005). In addition, the ATP-binding-dependent formation of ternary complexes between MutS and MutL (or their eukaryotic homologs) requires binding of the mispair recognition proteins to a mispaired base (Acharya et al., 2003; Blackwell et al., 2001; Mendillo et al., 2005). These mechanistic features amplify the specificity of mispair recognition. Regardless, the specificity of mispair binding in vitro is unlikely to account for the specificity of MMR in vivo.

One hypothesis for how mismatch recognition occurs in vivo is that MMR is coupled to DNA replication, which would localize MMR proteins to where mispaired bases are formed. Two lines of evidence suggest this. First, MMR in vitro requires single-strand breaks in the DNA (Iyer et al., 2006; Kunkel and Erie, 2005), suggesting that MMR might be targeted to strand breaks in the nascent DNA strands during DNA replication. Second, Msh2-Msh6 and Msh2-Msh3 (Clark et al., 2000; Flores-Rozas et al., 2000) as well as Mlh1-Pms1 (Dzantiev et al., 2004; Lee and Alani, 2006) complexes interact with the proliferating cell nuclear antigen (PCNA). Because PCNA is part of the replication machinery, these interactions could link MMR to DNA replication. Alternatively, because PCNA is left on the DNA after replication, binding of MMR proteins to PCNA could target MMR to regions of newly synthesized DNA (Shibahara and Stillman, 1999). However, the interaction between PCNA and Msh6 and Msh3 is not absolutely required for MMR (Flores-Rozas et al., 2000; Shell et al., 2007). Furthermore, PCNA is required at many steps during MMR including the activation of the human Pms2 (Pms1 in *S. cerevisiae*) endonuclease (Pluciennik et al., 2010) and the resynthesis step at the end of MMR (Gu et al., 1998; Umar et al., 1996). Therefore a PCNA requirement does not necessarily reflect coupling of MMR to DNA replication.

Here, we have used functional fluorescent-tagged MMR and replication proteins to study MMR in situ. Our results indicate that the Msh2-Msh6 mismatch recognition complex is an S phase component of replication centers independent of the presence of a mispaired base. Unexpectedly, Mlh1-Pms1 formed nuclear foci that, although dependent on Msh2-Msh6 for their formation, rarely colocalized with the Msh2-Msh6 replication-associated foci. The presence of mispaired bases or defects downstream of mispair recognition increased the formation of Mlh1-Pms1 foci but not Msh2-Msh6 foci. These findings suggest the presence of replication machinery-coupled and -independent pathways for mispair recognition by Msh2-Msh6, which in turn direct formation of superstoichiometric Mlh1-Pms1 foci that represent sites of active MMR.

RESULTS

Msh6 Forms Foci that Colocalize with Replication Factories

DNA replication in eukaryotic cells takes place at discrete globular foci or clusters within the S phase nucleus, sometimes referred to as replication factories (Hozák et al., 1993; Kitamura et al., 2006; Newport and Yan, 1996). To test for an association between MMR and DNA replication in live cells, we used deconvolution microscopy to image a variety of functional fluorescently tagged DNA replication and MMR proteins (Tables S1 and S2 available online; the replication proteins are essential and hence functional) expressed at normal levels (Figure S3A) from their native chromosomal loci in *S. cerevisiae*. Consistent with previous studies (Kitamura et al., 2006), Pol2-4GFP (catalytic subunit of DNA polymerase ε) formed multiple foci within the nucleus (Figure 1A). These foci were frequently observed in small or medium budded cells (S phase cells) and were essentially absent in unbudded cells (G1 cells) and cells with large buds (≥3 μm) (G2/M cells) (Figures 1A and 1B). Msh6-mCherry also formed nuclear foci (Figure 1A) that were more abundant in S phase cells (2.6 ± 1.4 [mean ± standard deviation (SD)], n = 103, foci per S phase cell) (Figures 1B and S1A). These Msh6-mCherry foci almost always colocalized with Pol2-4GFP foci (Figures 1A and 1B), suggesting that a portion of Msh2-Msh6 is present in replication factories. Importantly, a *rad52Δ* mutation that eliminates mitotic recombination, replication-dependent recombination intermediates and toxic recombination intermediates thought to arise from damaged replication forks (Fabre et al., 2002; Zou and Rothstein, 1997), and an *msh3Δ* mutation that eliminates targeting of Msh2 to recombination intermediates (Evans et al., 2000) did not significantly affect the frequency of Msh6 foci (Figure 2B).

We next tested colocalization of Msh6 with other replisome components including the following: Pol30 (PCNA), Pol3 (catalytic subunit of DNA polymerase δ), Pol1 (catalytic subunit of DNA polymerase α), Rfa1 (large subunit of replication protein A, RPA), and Mcm2 and Mcm4 (subunits of the MCM helicase complex Mcm2-7). Colocalization of Msh6 foci with Pol30, Pol3, and Pol1 foci was similar to that seen with Pol2 foci (Figure 1C). Rfa1 formed many foci, and Msh6 foci frequently colocalized with these, although a high percentage of Rfa1 foci did not colocalize with Msh6 foci. We could not detect colocalization of Msh6 with the MCM subunits Mcm2-4GFP, Mcm4-4GFP (Figure 1C), or Mcm7-4GFP (Figure S1B); Mcm7-mCherry also did not colocalize with Pol2-4GFP (Figure S1C). The lack of colocalization of MCM subunits with replication fork components in microscopy studies has been reported and remains a matter of discussion (Dimitrova et al., 1999; Laskey and Madine, 2003).

Msh2-Msh6 Foci Depend on Interaction with PCNA

We next tested whether colocalization of Msh6 with the replication machinery is mediated by an interaction with PCNA, via the PIP (*P*CNA *i*nteracting *p*rotein) box located at the N terminus of Msh6 (Clark et al., 2000; Flores-Rozas et al., 2000). An *msh6-F33AF34A*-GFP mutant, which disrupts the PIP box and the interaction with PCNA in vitro, displayed a severe reduction in the percentage of nuclei with Msh6-GFP foci in unsynchronized (Figures 2A and 2B) and S phase cells (Figures S2A and S2C). Similar results were obtained with the *msh6-2-51Δ* mutation that deletes the Msh6 PIP box and, like the *msh6-F33AF34A* mutation, causes only modest MMR defects (10%–15% reduction in MMR) (Shell et al., 2007). These results are consistent with prior observations in human cells transfected with a construct expressing a nonfunctional Msh6 lacking the first 77 N-terminal amino acids (*msh6-Δ77*) that does not interact with PCNA in vitro and also potentially in vivo (Kleczkowska

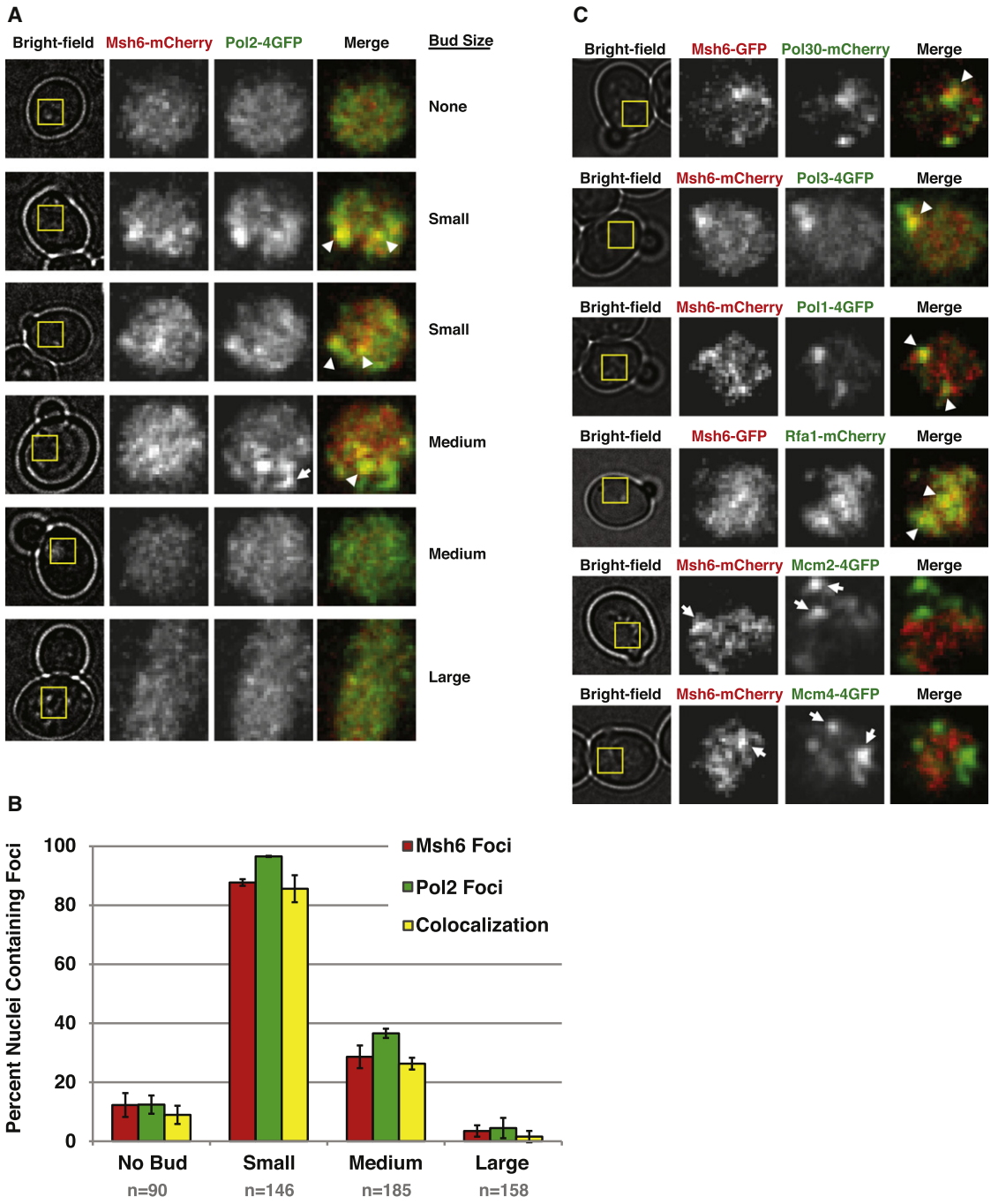

Figure 1. Msh2-Msh6 Forms Nuclear Foci that Colocalize with Replication Factories

Cells expressing Msh6-mCherry (or GFP) and a DNA replication-related protein tagged with 4GFP (or mCherry) were analyzed by deconvolution microscopy.

(A) Images of cells with different bud size expressing Msh6-mCherry and Pol2-4GFP.

(B) Distribution of Msh6-mCherry and Pol2-4GFP foci according to bud size: no bud or small (<1.5 μm), medium (1.5–3 μm), or large (>3 μm) budded cells. Error bars indicate standard error of the mean (SEM), and "n" indicates the number of cells examined.

(C) Msh6 colocalized with other components of the replisome including Pol30, Pol3, Pol1, and Rfa1 but not with the helicase subunits Mcm2 or Mcm4. Yellow boxes (2 μm square) in "Bright-field" correspond to the nucleus and were enlarged (without interpolation) for the fluorescent images. White arrows indicate mCherry/GFP foci, and arrowheads indicate colocalized foci on "Merge" images.

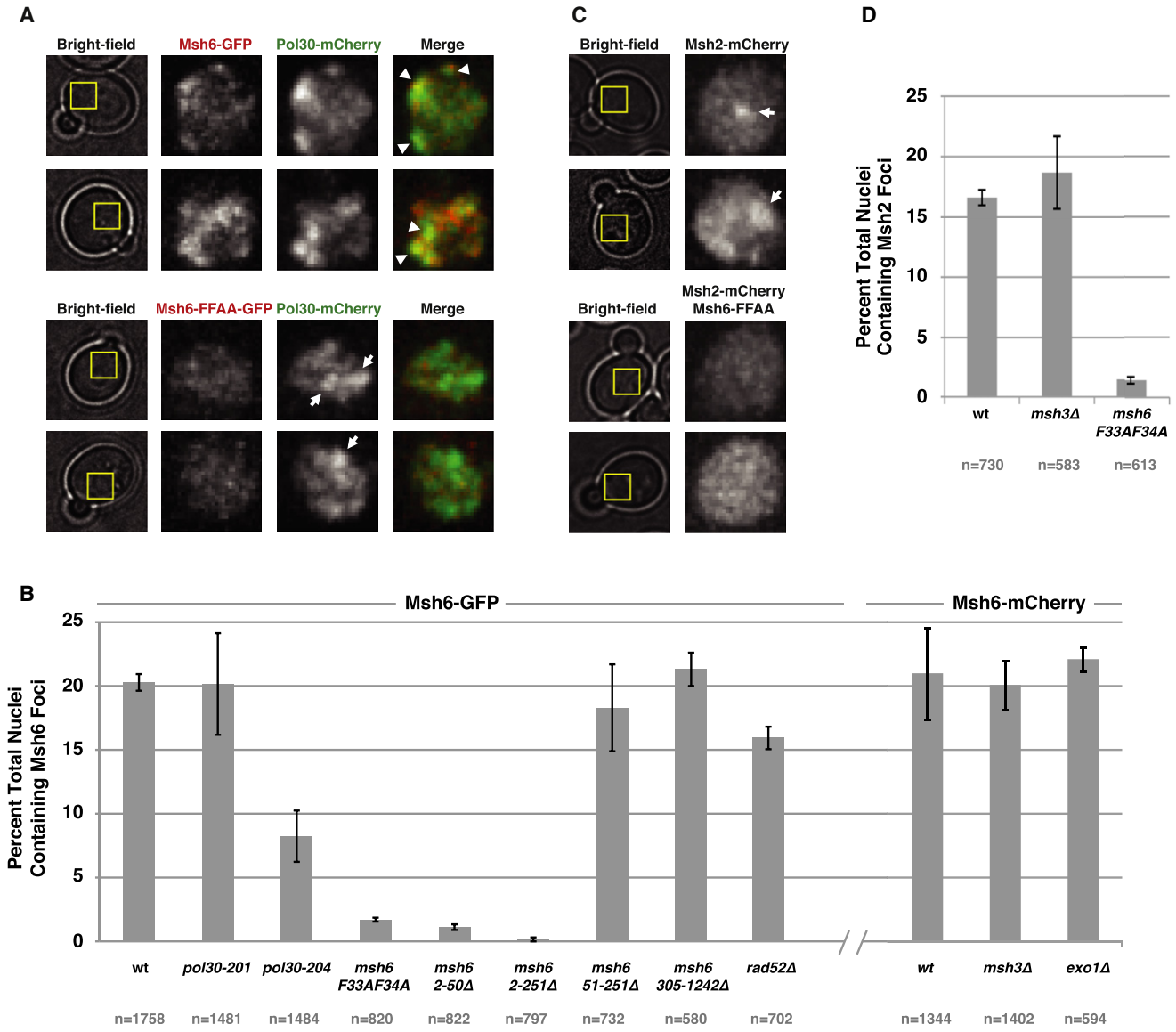

Figure 2. Msh2-Msh6 Replication-Associated Foci Depend on Interactions with PCNA

(A) Cells expressing Msh6-GFP or the Msh6-F33AF34A-GFP mutant protein were analyzed for colocalization with Pol30-mCherry.

(B) Quantification of the percentage of total nuclei containing Msh6-GFP or Msh6-mCherry foci for the indicated wild-type and mutant strains.

(C) Images of wild-type cells or the *msh6-F33AF34A* mutant expressing Msh2-mCherry.

(D) Quantification of the percentage of total nuclei containing Msh2-mCherry foci for the wild-type or *msh3Δ* or *msh6-F33AF34A* mutant.

Error bars indicate the SEM, and "n" indicates the number of cells examined (for B and D).

et al., 2001). We also quantified Msh6-GFP foci in a strain carrying the PCNA *pol30-204* allele (*pol30-C81R*) that results in a partial MMR defect and abolishes the ability of PCNA to interact with Msh2-Msh6 in vitro (Lau et al., 2002). This mutation caused an ~60% reduction in the percentage of cells with Msh6-GFP foci, whereas another partially MMR-defective *pol30* allele that does not alter the interaction of PCNA with Msh2-Msh6 in vitro, *pol30-201* (*pol30-C22Y*), had no effect on the frequency of Msh6-GFP foci. Furthermore, fusing GFP to the first 304 amino acids of Msh6, which comprise the unstructured Msh6 N-terminal region (Msh6-NTR) that by itself does not support MMR (Shell et al., 2007) (*msh6-305-1242Δ*-GFP), yielded foci at frequencies that were nearly identical to the frequency seen with Msh6-GFP (Figures 2B, S2A, and S2C), indicating that the Msh6-NTR is sufficient to interact with PCNA and form foci in vivo. These results show that Msh6 localizes to replication factories via an interaction with PCNA and that the PIP box is necessary and sufficient for this localization.

The Msh6-NTR has a second region that is important for MMR and that is partially redundant with the PIP box (Shell et al., 2007).

The *msh6-51-251Δ* mutation that deletes this second region and by itself only causes modest MMR defects (6% reduction in MMR) but does not compromise the PIP box or the Msh6-PCNA interaction did not affect Msh6-GFP foci formation (Figures 2B, S2A, and S2C). In contrast, the *msh6-2-251Δ* mutation that deletes both the Msh6 PIP box and this second region reduced the level of Msh6-GFP foci to the levels seen in the *msh6-F33AF34A* and *msh6-2-51Δ* PIP box mutants. In the case of only the *msh6-2-251Δ* mutation, some of the mutant protein was localized in the cytoplasm in addition to the nucleus. Mutations that eliminate the Msh6 PIP box cause only modest MMR defects (10%–15% reduction in MMR) by themselves but cause strong MMR defects in combination with the partially redundant *msh6-51-251Δ* mutation (Flores-Rozas et al., 2000; Shell et al., 2007). These results establish that the Msh6-PCNA interaction underlies Msh6 foci formation and makes a modest contribution to MMR in wild-type cells but is essential for MMR in the *msh6-51-251Δ* mutant.

Because eukaryotic cells have two partially redundant binding partners for Msh2 (Msh6 and Msh3) (Marsischky et al., 1996), we tested whether both Msh6 and Msh3 were able to target Msh2 to the replication factories. The frequency of Msh2-mCherry foci in wild-type cells was essentially the same as that seen for Msh6-GFP foci, and these were almost completely eliminated by an *msh6-F33AF34A* mutation that abolishes the interaction of Msh6 and PCNA in vitro (Clark et al., 2000; Flores-Rozas et al., 2000) (Figures 2C and 2D). In contrast, deletion of *MSH3*, which eliminates the function of Msh2-Msh3 in MMR and targeting of Msh2 to recombination intermediates (Evans et al., 2000), did not change the frequency of Msh2-mCherry foci (Figure 2D). These results indicate that the Msh2-mCherry foci in wild-type cells predominantly contain Msh2-Msh6. The inability to observe Msh2-mCherry foci in the *msh6-F33AF34A* mutant likely reflects the lower abundance of Msh3 compared to Msh6 (Genschel et al., 1998; Ghaemmaghami et al., 2003). We did not test the effect of deleting *MSH2* on the frequency of Msh6-GFP foci as loss of Msh2 is known to result in degradation of its binding partners, Msh6 and Msh3. Attempts to directly visualize Msh3 foci were unsuccessful, likely due to its low abundance.

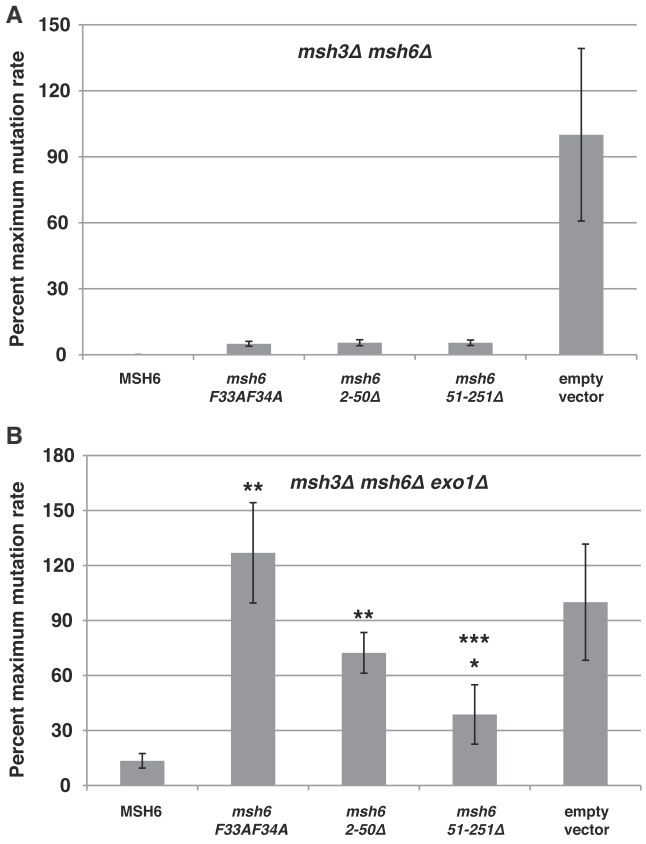

Figure 3. *MSH6* Mutants that Are Unable to Interact with PCNA Do Not Complement the Mutator Phenotype of an *msh3Δ msh6Δ exo1Δ* Strain

Mutation rates of *msh3Δ msh6Δ* (A) or *msh3Δ msh6Δ exo1Δ* (B) strains containing the indicated vector, MSH6 plasmid, or *MSH6*-NTR mutant plasmids were determined by fluctuation analysis using the *hom3-10* reversion assay. Rates are shown as a percentage relative to the maximum mutation rate (empty vector). Error bars indicate the SEM. * indicates p value < 0.001, and ** indicates p value > 0.15, both relative to the empty vector rate. *** indicates p value < 0.015 relative to the vector containing wild-type MSH6. Two-tailed p values were determined by Mann-Whitney tests.

Exo1 Is Preferentially Required for Msh6-PCNA Interaction-Independent MMR

Exo1 is a 5′-3′ exonuclease that physically interacts with Msh2 and Mlh1 (Schmutte et al., 2001; Tishkoff et al., 1997; Tran et al., 2001) and acts in the excision step of MMR in vitro (Dzantiev et al., 2004; Kadyrov et al., 2006; Zhang et al., 2005). Because deletion of *EXO1* results in a weaker mutator phenotype than deletion of *MSH2* and an *exo1Δ msh2Δ* double mutant has the same mutator phenotype as an *msh2Δ* single mutant, redundant factors likely exist (Tishkoff et al., 1997; Tran et al., 2001). In support of this, one study has identified mutations that only eliminate MMR in the absence of Exo1 (Amin et al., 2001). It has been suggested that either the DNA polymerase-associated editing exonucleases (Tran et al., 1999) or strand displacement DNA synthesis (Kadyrov et al., 2009) might substitute for Exo1. Consistent with a role for Exo1 downstream of mispair recognition (Genschel and Modrich, 2003; Kadyrov et al., 2006; Zhang et al., 2005), deletion of *EXO1* did not change the frequency of Msh6-mCherry foci (Figures 2B and S2C).

As the *exo1Δ* and *msh6-F33AF34A* mutations each cause weak mutator phenotypes and have different effects on Msh6 foci formation (Figure 2B), we investigated genetic interactions between these two mutations. We tested the ability of different *MSH6* mutant plasmids to complement the MMR defect of *msh3Δ msh6Δ* and *msh3Δ msh6Δ exo1Δ* mutants. As reported (Shell et al., 2007), plasmids carrying wild-type *MSH6*, *msh6-F33AF34A, msh6-2-50Δ*, and *msh6-51-251Δ* substantially complemented the high mutation rates of the MMR-defective *msh3Δ msh6Δ* mutant (Figure 3A). In contrast, plasmids containing the *msh6-F33AF34A* mutation or the *msh6-2-50Δ* deletion were completely defective for complementing the high mutation rates of the MMR-defective *msh3Δ msh6Δ exo1Δ* mutant (Figure 3B). On the other hand, plasmids carrying *MSH6* or the *msh6-51-251Δ* internal deletion (which does not compromise

Table 1. Mutation Rate Analysis of *exo1Δ* in Combination with *pol30-204* or with the Polymerase Mutant Alleles *pol2-M644G* and *pol3-L612M*

	Relevant Genotype	RDKY Strain	Mutation Rate (Fold Increase)[a] Thr$^+$	Can^R
A	Wild-type	3686	1.3 [0.5–1.8] × 10^{-9} (1)	4.3 [2.9–5.7] × 10^{-8} (1)
	exo1Δ	7532	4.1 [2.2–8.8] × 10^{-9} (3)	4.3 [3.1–6.1] × 10^{-7} (10)
	pol30-204	7539	2.6 [2.0–3.7] × 10^{-7} (200)	5.0 [4.4–14.0] × 10^{-7} (12)
	exo1Δ pol30-204	7531	7.3 [4.3–13.8] × 10^{-7} (562)	1.7 [1.2–2.0] × 10^{-6} (40)
	msh2Δ	5961	3.7 [3.0–5.2] × 10^{-6} (2846)	3.5 [3.0–4.5] × 10^{-6} (81)
B	*pol2-M644G*	7537	3.2 [2.1–] × 10^{-9} (3)	3.5 [2.6–5.2] × 10^{-7} (8)
	pol3-L612M	7538	3.1 [2.4–4.8] × 10^{-9} (2)	3.4 [2.6–5.2] × 10^{-7} (8)
	pol2-M644G exo1Δ	7533	4.1 [2.4–5.3] × 10^{-8} (32)	2.1 [1.6–2.7] × 10^{-6} (49)
	pol3-L612M exo1Δ	7534	3.6 [2.7–4.5] × 10^{-7} (277)	7.7 [5.8–9.8] × 10^{-6} (179)
	pol2-M644G msh2Δ	7535	2.8 [1.7–4.6] × 10^{-5} (21538)	5.5 [1.7–10.7] × 10^{-5} (1279)
	pol3-L612M msh2Δ	7536	4.4 [3.2–6.2] × 10^{-5} (33846)	7.5 [3.5–10.1] × 10^{-5} (1744)

[a] Median rates of *hom3-10* (Thr$^+$) reversion and inactivation of *CAN1* gene (Can^R) with 95% confidence interval in square brackets and fold increase relative to the wild-type in parentheses.

the PIP box) complemented the high mutation rates of the *msh3Δ msh6Δ exo1Δ* mutant. Consistent with these results, combining the *pol30-204* (*C81R*) mutation, which disrupts the Msh6-PCNA interaction, with an *exo1Δ* mutation also resulted in a synergistic increase in mutation rates (Table 1A). These results indicate that MMR is much more dependent on the Msh6-PCNA interaction in the absence of Exo1 than in the presence of Exo1 and that MMR involving the Msh6-PCNA interaction is at least partially redundant with Exo1-dependent MMR pathway(s).

Exo1 Is Preferentially Required for Lagging-Strand MMR

Because Exo1 is more important for Msh6-PCNA interaction-independent MMR than for Msh6-PCNA interaction-dependent MMR (Figure 3 and Table 1A), and because of the mechanistic differences between leading and lagging-strand DNA synthesis, we investigated the role of Exo1 in leading and lagging-strand MMR. We utilized the DNA polymerase mutations *pol2-M644G* and *pol3-L612M*, which cause increased misincorporation during leading and lagging-strand DNA replication, respectively (Nick McElhinny et al., 2007; Pursell et al., 2007). Combining an *exo1* deletion with the lagging-strand DNA polymerase *pol3-L612M* mutation resulted in a synergistic increase in mutation rate in the *hom3-10* frameshift reversion assay and the *CAN1* inactivation assay (Tables 1A and 1B) (Marsischky et al., 1996), consistent with the results observed when the *pol3-L612M* was combined with deletions of *MSH2* and *PMS1* (Li et al., 2005). Similarly, the nonessential lagging-strand polymerase subunit Pol32 was previously identified as being required for MMR in the absence of Exo1 but not in the presence of Exo1 (Amin et al., 2001). In contrast, unlike mutations in other MMR genes, combining an *exo1* deletion with the leading-strand DNA polymerase mutation *pol2-M644G* resulted in a much smaller increase in mutation rates (Tables 1A and 1B). These results suggest that lagging-strand MMR has a greater dependence on Exo1 than leading-strand MMR.

Pms1 Forms Foci that Rarely Colocalize with Msh6

After recognition of a mispair, Msh2-Msh6 and Msh2-Msh3 form ternary complexes with Mlh1-Pms1 (Blackwell et al., 2001; Habraken et al., 1997; Mendillo et al., 2005). We therefore determined whether replication-associated Msh6 foci also contain Mlh1-Pms1. We constructed a Pms1-4GFP that was functional in MMR even in combination with Msh6-mCherry (and in the absence of *MSH3*) (Table S2); however, all attempts to tag Mlh1 resulted in a nonfunctional protein (Smith et al., 2001). We therefore used Pms1-4GFP as a reporter for the Mlh1-Pms1 heterodimer in vivo (Prolla et al., 1994). Pms1-4GFP formed distinct nuclear foci, similar to Msh2 and Msh6, although at a significantly lower frequency of ~10% of logarithmically growing cells. Surprisingly, Pms1-4GFP foci rarely colocalized with Msh6-mCherry foci (Figures 4A and 4B) or Msh2-mCherry (data not shown). We also observed the same limited colocalization between Pms1-GFP and Msh6-mCherry or between Pms1-mCherry and Msh6-GFP (Figures S3D and S3E). This lack of colocalization suggests that the Pms1-4GFP foci were not present at replication factories. Consistent with this, Pms1-4GFP foci also did not colocalize with Rfa1-mCherry foci (Figure S3C).

We next tested whether the Pms1-4GFP foci were localized to specific compartments/structures within the nucleus using various nuclear structure markers, including Nic96 (nuclear periphery), Sik1 (nucleolus), Cse4 and Cbf2 (centromere), and the telomere-binding proteins Rap1, Rif1, Cdc13, and Sir3. Pms1-4GFP foci did not colocalize with any of these nuclear markers (Figure S3C and data not shown), suggesting that Pms1 foci represent a previously unidentified MMR intermediate.

Analysis of the distribution of the Pms1-4GFP and Msh6-mCherry foci according to bud size revealed that Pms1-4GFP foci were most abundant in small and medium budded cells, whereas Msh6-mCherry foci were mostly present in small budded cells (Figures 4A and 4B). Given that Msh6 is present at replication factories but rarely colocalizes with Pms1 foci, this suggests that Pms1 foci are formed later than Msh6 foci.

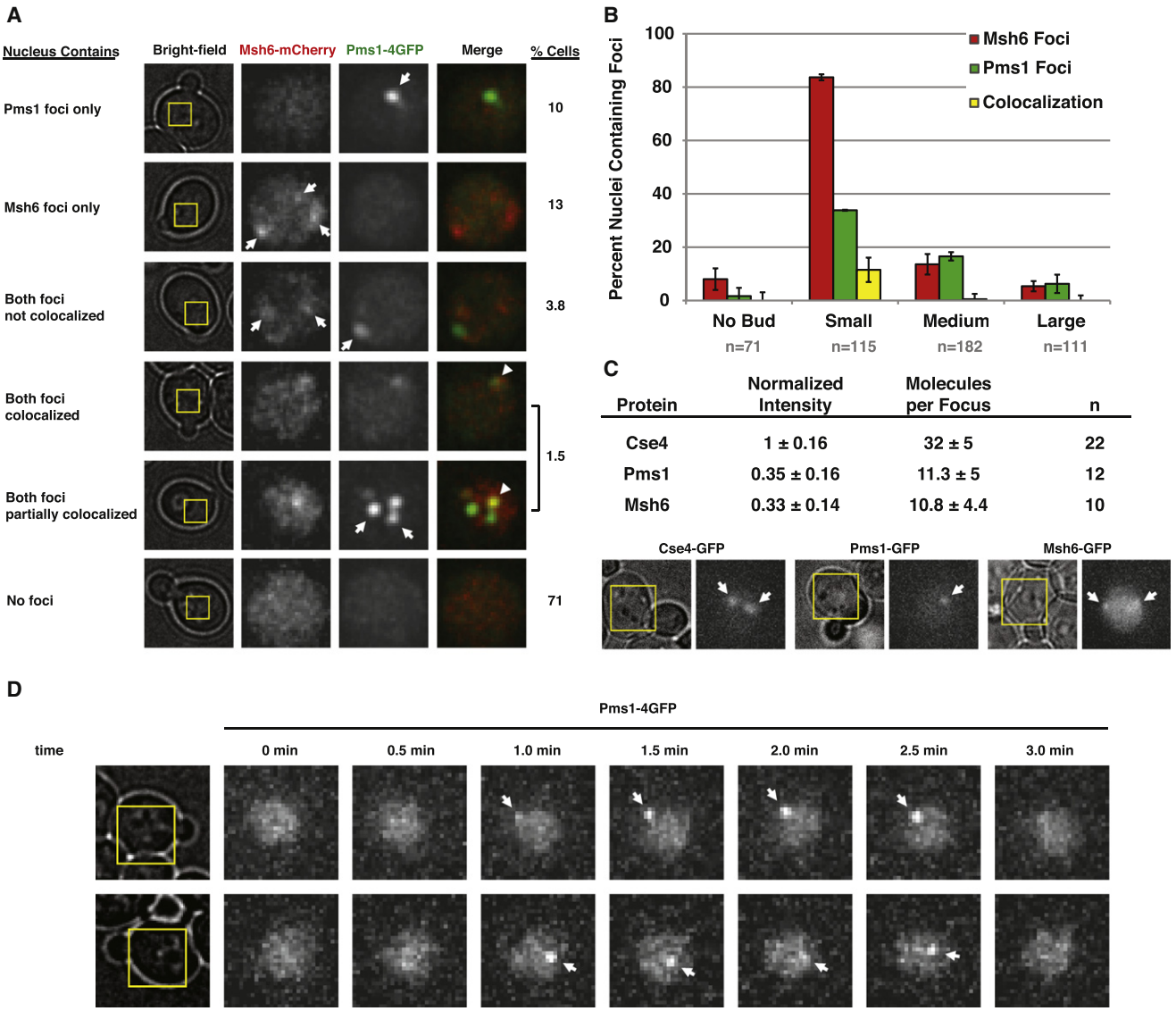

Figure 4. Pms1 Forms Foci that Rarely Colocalize with Msh6 Foci

(A) Cells expressing Msh6-mCherry and Pms1-4GFP were analyzed by deconvolution microscopy. Representative images illustrate Pms1-4GFP and Msh6-mCherry foci that do not colocalize, do colocalize, or partially colocalize.

(B) Distribution of the percentage of nuclei containing Msh6-mCherry or Pms1-4GFP foci according to bud size (bud-size categories were done as in Figure 1B). Error bars indicate the SEM, and "n" indicates the number of cells examined.

(C) Quantification of the average number of Msh6 or Pms1 molecules present per focus, using the centromere protein Cse4 as a standard.

(D) Time-lapse images of Pms1-4GFP were collected at the indicated intervals in a wild-type strain.

However, consistent with an S phase function, cells arrested in G2/M with nocodazole had few Msh6 and Pms1 foci, and a *clb2Δ* mutation that causes delay in G2/M and an increase in G2/M cells reduced the frequency of Msh6 and Pms1 foci (Figure S4A). After comparing the bud size distribution of Msh6-mCherry foci in the Pms1-4GFP colocalization experiment (Figure 4B) with the bud size distribution in the Pol2-4GFP colocalization experiment (Figure 1B), we noticed a small, reproducible reduction in the percentage of Msh6-mCherry foci, which was more evident in medium budded cells. We believe this difference may be due to a slight delay in S phase progression due to the presence of the 4GFP tag on Pol2.

The limited colocalization between Msh6 and Pms1 foci suggests that these two types of foci might represent different steps in the MMR reaction. To better understand these foci, we quantified the number of Msh6 or Pms1 molecules present in them using the centromere protein Cse4 as a fluorescence standard (Joglekar et al., 2006). Quantitative analysis of fluorescence intensity revealed that, on average, Pms1 foci contain 11 ± 5 molecules per focus (Figure 4C). Msh6 foci were more

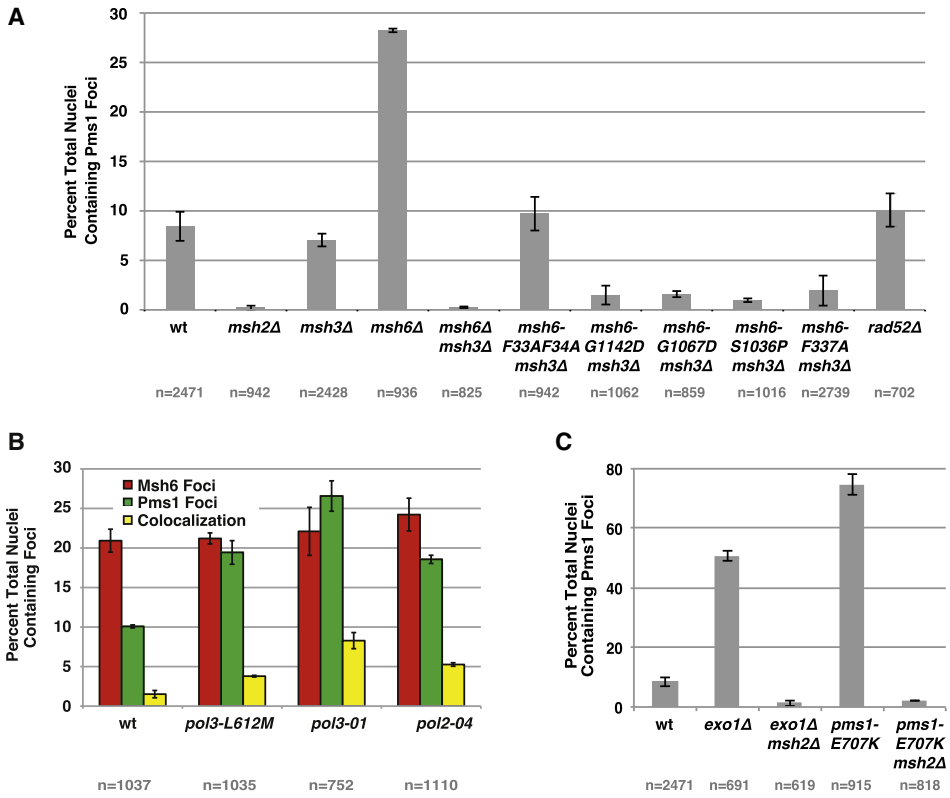

Figure 5. Pms1 Foci Are Sites of MMR

Pms1 foci were abolished in the absence of an Msh2-Msh6 complex and increased in response to induction of mispairs or downstream MMR-recognition defects.

(A) Quantification of the percentage of total nuclei containing Pms1-4GFP foci in the wild-type and indicated mutants.

(B) Percentage of total nuclei containing Msh6 and/or Pms1 foci (and colocalization) for strains expressing Msh6-mCherry and Pms1-4GFP in addition to the indicated polymerase mutations.

(C) Quantification of the Pms1-4GFP foci abundance for wild-type or *exo1Δ*, *exo1Δ msh2Δ*, *pms1-E707K*, or *pms1-E707K msh2Δ* mutants.

Error bars indicate the SEM, and "n" indicates the number of cells examined (for A–C).

difficult to quantify due to their less uniform nature. When the most distinctive Msh6 foci were quantified, they contained 11 ± 4 molecules per focus (Figure 4C). These measurements suggest that we should be able to visualize a focus containing 5–7 molecules of Msh6. The presence of Pms1 foci that are not coincident with Msh6 foci therefore suggests that Pms1 foci do not contain stoichiometric amounts of Msh6.

We also used time-lapse imaging to determine the average duration of a single Pms1-4GFP focus (Figure 4D). The Pms1-4GFP foci often showed rapid movements within the nucleus, indicating a dynamic behavior similar to that described for replication factories (Kitamura et al., 2006). The average duration of a single Pms1-4GFP focus was ~0.5–2.5 min (1.5 ± 1; mean ± SD, n = 88). MMR reactions require excision and resynthesis of relatively small tracks of mispair-containing DNA (up to 1 kb) (Fang and Modrich, 1993) and can be accomplished in vitro in about 15 min (Wang and Hays, 2002). Therefore, it is expected that in vivo, individual repair reactions might occur over a short period of time. The short lifetimes of Pms1-4GFP foci are therefore consistent with the idea that these foci represent an MMR intermediate.

Formation of Pms1 Foci Is Dependent on a Functional Msh2-Msh6 Complex

Given the low number of Pms1 foci in wild-type cells compared to the number of Msh6 foci and their limited colocalization, we tested whether upstream MMR components were required for the formation of Pms1-4GFP foci. Deletion of *MSH2*, which eliminates both the Msh2-Msh6 and Msh2-Msh3 mispair recognition complexes, largely eliminated the Pms1-4GFP foci (Figure 5A), and reintroduction of the *MSH2* gene on a low-copy plasmid restored Pms1-4GFP foci to wild-type levels (Figure S4B). Analysis of Pms1-4GFP protein levels in *msh2Δ* and wild-type strains revealed the same levels of Pms1-4GFP (Figure S4C), excluding the possibility that deletion of *MSH2* altered the levels of Pms1-4GFP. Deleting either *MSH3* or *MSH6* alone caused no reduction in the percentage of cells containing Pms1-4GFP foci (Figure 5A); in fact, there was a 2- to 3-fold increase in the frequency of Pms1-4GFP foci in the strain lacking Msh6. Simultaneous deletion of *MSH3* and *MSH6* almost completely eliminated the Pms1-4GFP foci, as observed following deletion of *MSH2* (Figure 5A). These results are consistent with the observed redundancy between the Msh6 and Msh3

subunits. Overall, these results indicate that Pms1-4GFP foci depend on the presence of mispair recognition complexes and that both the Msh2-Msh6 and Msh2-Msh3 complexes can promote the formation of Pms1 foci.

To address whether Pms1-4GFP foci were dependent on the formation of replication factory-associated Msh2-Msh6 foci, we introduced the *msh6-F33AF34A* mutation that abolishes Msh2-Msh6 foci formation (Figures 2A–2D) into an *msh3Δ* mutant strain expressing Pms1-4GFP. The *msh6-F33AF34A* mutation had no effect on the level of Pms1-4GFP foci (Figure 5A), indicating that although the formation of Pms1-4GFP foci in an *msh3Δ* mutant requires the Msh2-Msh6 complex, their formation was independent of the association of Msh2-Msh6 with PCNA.

We next analyzed the effects of the *msh6-G1142D*, *msh6-G1067D*, and *msh6-S1036P* mutations on the formation of Pms1-4GFP foci in an *msh3Δ* mutant. Each of these mutations results in normal levels (Figure S3B) of an Msh2-Msh6 complex that recognizes mispaired bases normally; however, the Msh2-Msh6-G1142D complex forms ternary complexes with Mlh1-Pms1 but is defective for sliding clamp formation, whereas the Msh2-Msh6-G1067D and Msh2-Msh6-S1036P complexes are defective for both sliding clamp formation and assembly of Mlh1-Pms1 ternary complexes (Hargreaves et al., 2010; Hess et al., 2006). Each of these *msh6* mutations reduced the level of Pms1-4GFP foci to the same levels seen in the *msh2Δ* single mutant and the *msh3Δ msh6Δ* double mutant (Figure 5A). These results indicate that the ability of Msh2-Msh6 to recognize mispaired bases and bind Mlh1-Pms1 is not sufficient for Msh2-Msh6 to support the formation of Pms1-4GFP foci; in addition to these activities, the conformational change underlying the ability of Msh2-Msh6 to form a sliding clamp is required. Cumulatively, these results indicate that despite their limited colocalization with replication factory-associated mispair recognition complex foci, the formation of Pms1 foci requires the Msh2-Msh6 or the Msh2-Msh3 complex.

Pms1 Foci Increase in Response to Induction of Mispaired Bases

If Pms1-4GFP foci represent active sites of MMR, their frequency should respond to increased levels of mispaired bases. To test this, we used three DNA polymerase mutations that cause increased misincorporation rates either due to a mutation at the polymerase active site (*pol3-L612M*) (Li et al., 2005; Nick McElhinny et al., 2008; Pursell et al., 2007) or due to inactivation of the 3′ exonuclease proofreading activity (*pol2-04* and *pol3-01*) (Morrison et al., 1991, 1993). All three mutations caused a significant (2- to 3-fold) increase in the percentage of nuclei containing Pms1-4GFP foci (Figure 5B). Furthermore, formation of Pms1-4GFP foci in the *pol3-L612M* and *pol2-04* mutants was *MSH2* dependent (Figure S4D); we were unable to analyze the *MSH2* dependence of Pms1-4GFP foci in the *pol3-01* mutant as *pol3-01* is lethal in combination with an *msh2Δ* mutation (Morrison et al., 1993; Tran et al., 1999). These observations indicate that Pms1 foci increase when mispairs increase and support the idea that Pms1 foci represent active sites of MMR. Consistent with this, when present in an *msh3Δ* mutant, the *msh6-F337A* mutation that eliminates mispair binding (Bowers et al., 2000) reduced the Pms1 foci (Figure 5A), whereas a *rad52Δ* mutation, which eliminates recombination intermediates (Zou and Rothstein, 1997), did not affect the frequency of Pms1 foci (Figure 5A).

We next analyzed whether the increased misincorporation rates caused by the *pol3-L612M*, *pol2-04*, and *pol3-01* mutations would increase colocalization of Msh6-mCherry foci with Pms1-4GFP foci. The three mutations had no effect on the abundance of Msh6-mCherry foci and only caused a modest increase in the percentage of cells with colocalized Pms1-4GFP and Msh6-mCherry foci, which may simply reflect the overall increase in Pms1-4GFP foci abundance in these three mutants (Figure 5B). Overall, these data suggest that Msh6 foci are present at replication factories at constitutive levels, whereas Pms1 foci rarely colocalize with replication factory-associated Msh6 foci. Instead, the abundance of Pms1 foci appears to be determined by the frequency of mispairs generated by DNA polymerases that are then detected by the mispair recognition complexes.

MMR Defects downstream of Mlh1-Pms1 Recruitment Increase the Level of Pms1 Foci

To further characterize the properties of Pms1 foci, we tested the effect of inhibiting MMR downstream of Mlh1-Pms1 on the prevalence of Pms1-4GFP foci. Deletion of *EXO1* resulted in a 5-fold increase in the percentage of cells containing Pms1-4GFP foci, and these foci were *MSH2* dependent (Figure 5C). In addition, deletion of *EXO1* also increased the number of Pms1-4GFP foci per nucleus (Figure S4E). Consistent with the role of Exo1 downstream of mispair recognition, deletion of *EXO1* did not have any effect on the percentage of cells containing Msh6-mCherry foci (Figure 2B).

Human Pms2 (Pms1 in *S. cerevisiae*) has an endonuclease activity required for MMR (Kadyrov et al., 2006; Pluciennik et al., 2010). The human *pms2-E705K* mutation (analogous to *S. cerevisiae pms1-E707K*) changes an amino acid located in the conserved motif $DQHA(X)_2E(X)_4E$, abolishes the endonuclease function of Pms2, and results in a defect in MMR (Kadyrov et al., 2006). The *pms2-E705K* mutation does not affect upstream steps during MMR, including mispair recognition and assembly of Msh2-Msh6-Mlh1-Pms2 ternary complexes (Kadyrov et al., 2006). As the equivalent *S. cerevisiae pms1-E707K* mutation also results in an MMR defect (Deschênes et al., 2007; Kadyrov et al., 2007), we tested the effect of the *pms1-E707K* mutation on the abundance of Pms1-4GFP foci. Introduction of the *pms1-E707K* mutation resulted in a 7-fold increase in the percentage of cells with Pms1-4GFP foci, which were *MSH2* dependent (Figure 5C). These results are consistent with the idea that, when the downstream Exo1 or Pms1 endonuclease functions are compromised, Mlh1-Pms1 complexes do not turn over, resulting in higher levels of Pms1-4GFP foci.

DISCUSSION

Much of our knowledge about MMR comes from genetic studies and in vitro reconstitution experiments. Although a few attempts to visualize MMR proteins under conditions of normal DNA replication in vivo have been reported, these studies have been complicated by the use of overexpressed levels of MMR proteins (Elez et al., 2010) or the use of partially functional or nonfunctional tagged MMR proteins (Smith et al., 2001) and only report

a limited analysis (Elez et al., 2010; Kleczkowska et al., 2001; Smith et al., 2001). Here, we used fully functional GFP- or mCherry-tagged versions of the MMR proteins Msh2, Msh6, and Pms1, expressed at native levels, to visualize Msh2-Msh6 and Mlh1-Pms1 complexes in living *S. cerevisiae* cells. We found that Msh2-Msh6 formed nuclear foci in S phase cells that colocalized with replication factories. This colocalization was completely dependent on the interaction between the Msh6 N-terminal PIP box and PCNA, and the N terminus of Msh6 was sufficient for this interaction. Mutations in *POL2* and *POL3* that increase the frequency of mispairs, a *rad52Δ* mutation that eliminates recombination and replication-dependent recombination intermediates, and an *msh3Δ* mutation that eliminates targeting of Msh2 to recombination intermediates did not affect the frequency of Msh2-Msh6 foci. In addition, Rad52 foci, which form at recombination and repair intermediates, occur in S phase cells at less than 10% of the frequency of Msh2-Msh6 foci (Lisby et al., 2001). Therefore, Msh2-Msh6 foci are not assembled in response to mispaired bases or recombination and repair intermediates but represent a mispair recognition system that is constitutively present as an integral component of a significant proportion of replication factories.

The formation of Msh2-Msh6 foci and their localization to replication factories depended on the interaction between the PIP box at the Msh6 N terminus and PCNA. However, mutations that eliminate the interaction between Msh6 and PCNA only cause a 10%–15% reduction in the efficiency of MMR. These results suggest that there are additional redundant pathway(s) for mispair recognition that do not involve the formation of Msh2-Msh6 foci coupled to replication factories. These alternative pathways require Exo1 and an internal region of the Msh6 N-terminal leader sequence, as MMR in *exo1Δ* and *msh6-51-251Δ* mutants was completely dependent on the interaction between Msh6 and PCNA. The observation that the MMR pathway coupled to DNA replication becomes essential for preventing the accumulation of mutations in the absence of Exo1 is consistent with the previous identification of mutations that inactivate MMR only in the absence of Exo1 (Amin et al., 2001), one of which was a deletion of *POL32* that encodes a nonessential subunit of DNA polymerase δ. Furthermore, lagging-strand MMR was significantly more dependent on *EXO1* than leading-strand MMR, providing additional evidence for a specific MMR pathway(s) that depends on Exo1. An alternative explanation is that *EXO1* deletion and Msh6-PCNA interaction-defective mutants exhibit a synergistic MMR defect by extending the time that is required to complete MMR past the time it takes to reinitiate S phase in the next cell cycle.

We also used live-cell imaging to visualize MMR proteins that function downstream from mismatch recognition. We found that Mlh1-Pms1 also formed distinct S phase nuclear foci, but these foci rarely colocalized with Msh2-Msh6 foci or replication factories and did not colocalize with telomeres, centromeres, the nucleolus, or the nuclear periphery. Four main lines of evidence indicate that these Mlh1-Pms1 foci represent sites where active MMR is taking place. First, Mlh1-Pms1 foci were completely abolished by mutations that eliminate the Msh2-Msh6 and Msh2-Msh3 mispair recognition complexes or mispair recognition. In addition, *msh6* mutations that do not affect mispair recognition but prevent sliding clamp formation and the interaction with Mlh1-Pms1 eliminated the Mlh1-Pms1 foci. Second, the frequency of Mlh1-Pms1 foci was increased by mutations in *POL2* or *POL3* that increase the frequency of mispaired bases in cells. Third, mutations that inactivate MMR downstream of the interaction of Mlh1-Pms1 with Msh2-Msh6, including a Pms1 endonuclease mutation and an *exo1Δ* mutation, resulted in increased levels of Mlh1-Pms1 foci. Fourth, a *rad52Δ* mutation that eliminates recombination and replication-dependent recombination intermediates had no effect on Pms1 foci. These results are consistent with Mlh1-Pms1 foci being an active intermediate during MMR.

The observation that Mlh1-Pms1 foci do not colocalize with Msh2-Msh6 foci or contain substoichiometric amounts of Msh2-Msh6 that are below the limits of detection was surprising. One possible explanation for this is that the action, or a step in the action, of Mlh1-Pms1 in MMR is temporally separable from the mispair-dependent interaction of Msh2-Msh6 with Mlh1-Pms1 during MMR. Alternatively, once a mispaired base is recognized by Msh2-Msh6, one or a few molecules of Msh2-Msh6 catalytically load multiple Mlh1-Pms1 complexes onto the DNA, resulting in the formation Mlh1-Pms1 foci. These mechanisms are inconsistent with previous ideas proposing that multiple Msh2-Msh6 complexes are recruited at the mispair site, with each one of them able to interact with one Mlh1-Pms1 heterodimer. A number of studies have reported that MutL and Mlh1-Pms1 can interact with DNA, although the biological significance of this has been questioned (Park et al., 2010); however, the correlation of Mlh1-Pms1 foci with mispair levels suggests that the interaction of Mlh1-Pms1 with DNA may reflect a mechanistic step in MMR.

We found that the *msh6-G1142D* mutation, which results in a mutant Msh2-Msh6 complex that forms mispair-dependent ternary complexes with Mlh1-Pms1 but does not form sliding clamps, eliminated the formation of Mlh1-Pms1 foci. This result indicates that the ability of Msh2-Msh6 to interact with Mlh1-Pms1 is not sufficient for Mlh1-Pms1 foci formation. Rather, it is likely that conformational changes of Msh2-Msh6 that occur after mismatch recognition and Mlh1-Pms1 recruitment are essential for loading multiple Mlh1-Pms1 complexes. We speculate that loading of multiple Mlh1-Pms1 complexes at the site of the mispair is a crucial step necessary to guarantee the subsequent degradation and repair of the mispair-containing strand. This mechanism shares similarities with the one proposed for double-strand break repair, where phosphorylation of several H2A histone molecules (ϒ-H2AX) adjacent to the site of the break marks and amplifies the signal to ensure subsequent repair.

A model summarizing our results is presented in Figure 6. In this model, Msh2-Msh6 can locate mismatches in two ways. The first is as a component of replication factories, where it acts as a sensor coupled to DNA replication by PCNA. Because DNA replication mediates the disassembly of chromatin, this coupling of MMR to replication provides a mechanism by which MMR is able to overcome the barriers to repair presented by chromatin structure. Alternatively, Msh2-Msh6 can scan the genome for mispairs independently of its association with replication factories. The nature of this second pathway is unclear. When a mispair is encountered, Msh2-Msh6 loads multiple

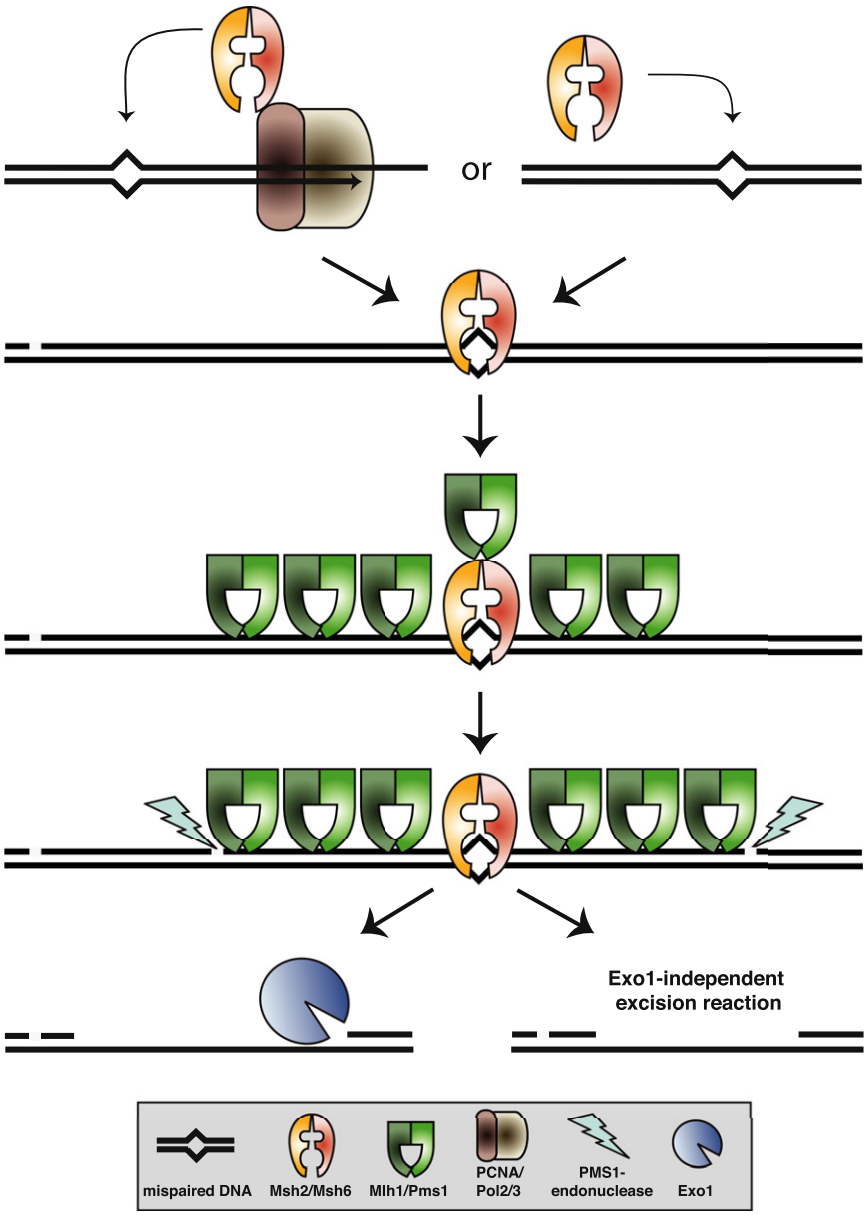

Figure 6. Model of MMR Pathways

Replication- and repair-associated foci are intermediates of MMR. At least two independent pathways act in preventing the accumulation of mispairs; one is coupled to the replication machinery through the interaction between Msh6 and PCNA and acts as a sensor of potential mispairs. An alternative pathway might exist that does not require the Msh2-Msh6 association to replication factories. After mispair recognition, Msh2-Msh6 is able to recruit multiple molecules of Mlh1-Pms1 to the site of the mispair. This is followed by activation of the endonuclease activity of Pms1 and Exo1 recruitment. Inactivation of either of these two last steps might lead to an accumulation of these Pms1 foci intermediates.

molecules of Mlh1-Pms1 onto DNA, Mlh1-Pms1 is activated, and Exo1, or other excision functions, is recruited for removal of the mispair-containing DNA strand followed by DNA resynthesis and ligation. The ability to visualize and quantify MMR intermediates provides an assay that can be used for identification and analysis of MMR components in the alternative MMR pathways.

EXPERIMENTAL PROCEDURES

Media, Strains, and Plasmids

S. cerevisiae strains were grown at 30°C in yeast extract-peptone-dextrose media (YPD) or appropriate dextrose synthetic dropout media for selection of plasmid markers and/or Lys^+ or Thr^+ revertants or canavanine-resistant (Can^R) mutants. All strains used in this study (see Table S1) were derivatives of the S288C strain RDKY3686 *MATα ura3-52 leu2Δ1 trp1Δ63 his3Δ200 hom3-10 lys2-10A* (Amin et al., 2001). Gene deletions or tagging were performed using standard PCR-based recombination methods followed by confirmation by PCR. Correct insertion of tags, as well as absence of additional mutations, was confirmed by sequencing. Specific point mutations (*msh6-G1142D, msh6-G1067D, msh6-S1036P, msh6-F337A, pms1-E707K, pol30-201, pol30-204, pol2-04, pol2-M644G, pol3-01*, and *pol3-L612M*) were introduced via the integration/excision method using integrating plasmids (see Extended Experimental Procedures), and the presence of the desired mutation and absence of additional mutations were confirmed by DNA sequencing.

The *msh6-NTR* mutant alleles (*msh6-F33AF34A*, *msh6-2-50Δ*, *msh6-51-251Δ*, *msh6-2-251Δ*) were also expressed on a low-copy number plasmid (Shell et al., 2007) to test their ability to complement the MMR defects of the RDKY4234 and RDKY7203 strains.

For microscopy studies, the C terminus of the protein of interest was fluorescently tagged at the endogenous gene locus with the green fluorescent protein (GFP) or the red fluorescent protein (mCherry), except in the case of low-abundance proteins (i.e., Pol1, Pol2, Pol3, and in some cases Pms1) that were tagged with four tandem copies of GFP (4GFP) using the pSM1023 plasmid (gift of E. Schiebel). Because the DNA replication proteins analyzed in the present study are essential, the absence of growth defects indicates that these tagged proteins retain their functionality. Strains expressing the tagged mismatch repair proteins were tested using mutator assays, which indicated that C-terminal tagging of Msh2, Msh6, or Pms1 did not compromise their functionality (Table S2).

Immunoblotting

S. cerevisiae whole-cell extracts were analyzed by 4%–15% SDS-PAGE (Bio-Rad) and immunoblotting using anti-GFP or anti-Msh6 antibodies. Pgk1 was monitored as loading control.

Genetic Assays

Mutation rates were determined using the *hom3-10* and *lys2-10A* frameshift reversion and *CAN1* inactivation assays by fluctuation analysis (Amin

et al., 2001; Marsischky et al., 1996). Mann-Whitney tests were performed (http://faculty.vassar.edu/lowry/utest.html), and 95% confidence intervals were calculated to evaluate statistical significance.

Live-Cell Imaging and Image Analysis

Exponentially growing cultures were washed and resuspended in water, placed on minimal media agar pads, covered with a coverslip, and imaged on a Deltavision (Applied Precision) microscope with an Olympus 100× 1.35NA objective. Fourteen 0.5 μm z sections were acquired and deconvolved with softWoRx software. Experiments involving fluorescence quantification were done as described previously (Joglekar et al., 2006). Further image processing, including maximum intensity projections and intensity measurements were performed using ImageJ. Msh6-Pms1 colocalization was scored if at least one focus per nucleus displayed colocalization in the same z section. Msh6-Pol2 colocalization and colocalization with other replication proteins were scored if at least half of the Msh6 foci in a nucleus colocalized with Pol2 foci. Images with the same fluorescent fusion protein in the same figure have identical contrast adjustment.

Extended Experimental Procedures and a strain list are available in the Supplemental Information.

SUPPLEMENTAL INFORMATION

Supplemental Information includes Extended Experimental Procedures, four figures, and two tables and can be found with this article online at doi:10.1016/j.cell.2011.10.025.

ACKNOWLEDGMENTS

The authors would like to thank Kolodner and Desai Lab members for discussions; T. Kunkel, S. Martinez, M. Mendillo, L. Reha-Krantz, E. Schiebel, S. Shell, R. Tsien, and the Yeast Resource Center for providing plasmids/strains; S. Sandall for initial technical microscopy support; and C. Putnam and R. Fishel for discussions and comments on the manuscript. This work was supported by NIH grants GM50006 and GM085764 (R.D.K.), GM074215 (A.D.), and CA23100 (A.D., R.D.K.) and a Damon Runyon Cancer Research Foundation Fellowship (C.S.C.).

Received: April 20, 2011
Revised: July 22, 2011
Accepted: October 7, 2011
Published: November 23, 2011

REFERENCES

Acharya, S., Foster, P.L., Brooks, P., and Fishel, R. (2003). The coordinated functions of the E. coli MutS and MutL proteins in mismatch repair. Mol. Cell *12*, 233–246.

Alani, E. (1996). The Saccharomyces cerevisiae Msh2 and Msh6 proteins form a complex that specifically binds to duplex oligonucleotides containing mismatched DNA base pairs. Mol. Cell. Biol. *16*, 5604–5615.

Amin, N.S., Nguyen, M.N., Oh, S., and Kolodner, R.D. (2001). exo1-Dependent mutator mutations: model system for studying functional interactions in mismatch repair. Mol. Cell. Biol. *21*, 5142–5155.

Blackwell, L.J., Wang, S., and Modrich, P. (2001). DNA chain length dependence of formation and dynamics of hMutSalpha.hMutLalpha.heteroduplex complexes. J. Biol. Chem. *276*, 33233–33240.

Bowers, J., Tran, P.T., Liskay, R.M., and Alani, E. (2000). Analysis of yeast MSH2-MSH6 suggests that the initiation of mismatch repair can be separated into discrete steps. J. Mol. Biol. *302*, 327–338.

Cannavo, E., Marra, G., Sabates-Bellver, J., Menigatti, M., Lipkin, S.M., Fischer, F., Cejka, P., and Jiricny, J. (2005). Expression of the MutL homologue hMLH3 in human cells and its role in DNA mismatch repair. Cancer Res. *65*, 10759–10766.

Clark, A.B., Valle, F., Drotschmann, K., Gary, R.K., and Kunkel, T.A. (2000). Functional interaction of proliferating cell nuclear antigen with MSH2-MSH6 and MSH2-MSH3 complexes. J. Biol. Chem. *275*, 36498–36501.

Datta, A., Adjiri, A., New, L., Crouse, G.F., and Jinks Robertson, S. (1996). Mitotic crossovers between diverged sequences are regulated by mismatch repair proteins in Saccaromyces cerevisiae. Mol. Cell. Biol. *16*, 1085–1093.

Deschênes, S.M., Tomer, G., Nguyen, M., Erdeniz, N., Juba, N.C., Sepúlveda, N., Pisani, J.E., and Liskay, R.M. (2007). The E705K mutation in hPMS2 exerts recessive, not dominant, effects on mismatch repair. Cancer Lett. *249*, 148–156.

Dimitrova, D.S., Todorov, I.T., Melendy, T., and Gilbert, D.M. (1999). Mcm2, but not RPA, is a component of the mammalian early G1-phase prereplication complex. J. Cell Biol. *146*, 709–722.

Dzantiev, L., Constantin, N., Genschel, J., Iyer, R.R., Burgers, P.M., and Modrich, P. (2004). A defined human system that supports bidirectional mismatch-provoked excision. Mol. Cell *15*, 31–41.

Elez, M., Murray, A.W., Bi, L.J., Zhang, X.E., Matic, I., and Radman, M. (2010). Seeing mutations in living cells. Curr. Biol. *20*, 1432–1437.

Evans, E., Sugawara, N., Haber, J.E., and Alani, E. (2000). The Saccharomyces cerevisiae Msh2 mismatch repair protein localizes to recombination intermediates in vivo. Mol. Cell *5*, 789–799.

Fabre, F., Chan, A., Heyer, W.D., and Gangloff, S. (2002). Alternate pathways involving Sgs1/Top3, Mus81/ Mms4, and Srs2 prevent formation of toxic recombination intermediates from single-stranded gaps created by DNA replication. Proc. Natl. Acad. Sci. USA *99*, 16887–16892.

Fang, W.H., and Modrich, P. (1993). Human strand-specific mismatch repair occurs by a bidirectional mechanism similar to that of the bacterial reaction. J. Biol. Chem. *268*, 11838–11844.

Flores-Rozas, H., and Kolodner, R.D. (1998). The Saccharomyces cerevisiae MLH3 gene functions in MSH3-dependent suppression of frameshift mutations. Proc. Natl. Acad. Sci. USA *95*, 12404–12409.

Flores-Rozas, H., Clark, D., and Kolodner, R.D. (2000). Proliferating cell nuclear antigen and Msh2p-Msh6p interact to form an active mispair recognition complex. Nat. Genet. *26*, 375–378.

Genschel, J., and Modrich, P. (2003). Mechanism of 5′-directed excision in human mismatch repair. Mol. Cell *12*, 1077–1086.

Genschel, J., Littman, S.J., Drummond, J.T., and Modrich, P. (1998). Isolation of MutSbeta from human cells and comparison of the mismatch repair specificities of MutSbeta and MutSalpha. J. Biol. Chem. *273*, 19895–19901.

Ghaemmaghami, S., Huh, W.K., Bower, K., Howson, R.W., Belle, A., Dephoure, N., O'Shea, E.K., and Weissman, J.S. (2003). Global analysis of protein expression in yeast. Nature *425*, 737–741.

Gradia, S., Subramanian, D., Wilson, T., Acharya, S., Makhov, A., Griffith, J., and Fishel, R. (1999). hMSH2-hMSH6 forms a hydrolysis-independent sliding clamp on mismatched DNA. Mol. Cell *3*, 255–261.

Gu, L., Hong, Y., McCulloch, S., Watanabe, H., and Li, G.M. (1998). ATP-dependent interaction of human mismatch repair proteins and dual role of PCNA in mismatch repair. Nucleic Acids Res. *26*, 1173–1178.

Habraken, Y., Sung, P., Prakash, L., and Prakash, S. (1997). Enhancement of MSH2-MSH3-mediated mismatch recognition by the yeast MLH1-PMS1 complex. Curr. Biol. *7*, 790–793.

Hargreaves, V.V., Shell, S.S., Mazur, D.J., Hess, M.T., and Kolodner, R.D. (2010). Interaction between the Msh2 and Msh6 nucleotide-binding sites in the Saccharomyces cerevisiae Msh2-Msh6 complex. J. Biol. Chem. *285*, 9301–9310.

Hess, M.T., Mendillo, M.L., Mazur, D.J., and Kolodner, R.D. (2006). Biochemical basis for dominant mutations in the Saccharomyces cerevisiae MSH6 gene. Proc. Natl. Acad. Sci. USA *103*, 558–563.

Hozák, P., Hassan, A.B., Jackson, D.A., and Cook, P.R. (1993). Visualization of replication factories attached to nucleoskeleton. Cell *73*, 361–373.

Huang, S.N., and Crothers, D.M. (2008). The role of nucleotide cofactor binding in cooperativity and specificity of MutS recognition. J. Mol. Biol. *384*, 31–47.

Iaccarino, I., Marra, G., Palombo, F., and Jiricny, J. (1998). hMSH2 and hMSH6 play distinct roles in mismatch binding and contribute differently to the ATPase activity of hMutSalpha. EMBO J. *17*, 2677–2686.

Iyer, R.R., Pluciennik, A., Burdett, V., and Modrich, P.L. (2006). DNA mismatch repair: functions and mechanisms. Chem. Rev. *106*, 302–323.

Jiricny, J., Su, S.S., Wood, S.G., and Modrich, P. (1988). Mismatch-containing oligonucleotide duplexes bound by the E. coli mutS-encoded protein. Nucleic Acids Res. *16*, 7843–7853.

Joglekar, A.P., Bouck, D.C., Molk, J.N., Bloom, K.S., and Salmon, E.D. (2006). Molecular architecture of a kinetochore-microtubule attachment site. Nat. Cell Biol. *8*, 581–585.

Kadyrov, F.A., Dzantiev, L., Constantin, N., and Modrich, P. (2006). Endonucleolytic function of MutLalpha in human mismatch repair. Cell *126*, 297–308.

Kadyrov, F.A., Holmes, S.F., Arana, M.E., Lukianova, O.A., O'Donnell, M., Kunkel, T.A., and Modrich, P. (2007). Saccharomyces cerevisiae MutLalpha is a mismatch repair endonuclease. J. Biol. Chem. *282*, 37181–37190.

Kadyrov, F.A., Genschel, J., Fang, Y., Penland, E., Edelmann, W., and Modrich, P. (2009). A possible mechanism for exonuclease 1-independent eukaryotic mismatch repair. Proc. Natl. Acad. Sci. USA *106*, 8495–8500.

Kitamura, E., Blow, J.J., and Tanaka, T.U. (2006). Live-cell imaging reveals replication of individual replicons in eukaryotic replication factories. Cell *125*, 1297–1308.

Kleczkowska, H.E., Marra, G., Lettieri, T., and Jiricny, J. (2001). hMSH3 and hMSH6 interact with PCNA and colocalize with it to replication foci. Genes Dev. *15*, 724–736.

Kolodner, R. (1996). Biochemistry and genetics of eukaryotic mismatch repair. Genes Dev. *10*, 1433–1442.

Kolodner, R.D., and Marsischky, G.T. (1999). Eukaryotic DNA mismatch repair. Curr. Opin. Genet. Dev. *9*, 89–96.

Kunkel, T.A., and Erie, D.A. (2005). DNA mismatch repair. Annu. Rev. Biochem. *74*, 681–710.

Lang, G.I., and Murray, A.W. (2008). Estimating the per-base-pair mutation rate in the yeast Saccharomyces cerevisiae. Genetics *178*, 67–82.

Laskey, R.A., and Madine, M.A. (2003). A rotary pumping model for helicase function of MCM proteins at a distance from replication forks. EMBO Rep. *4*, 26–30.

Lau, P.J., Flores-Rozas, H., and Kolodner, R.D. (2002). Isolation and characterization of new proliferating cell nuclear antigen (POL30) mutator mutants that are defective in DNA mismatch repair. Mol. Cell. Biol. *22*, 6669–6680.

Lee, S.D., and Alani, E. (2006). Analysis of interactions between mismatch repair initiation factors and the replication processivity factor PCNA. J. Mol. Biol. *355*, 175–184.

Li, L., Murphy, K.M., Kanevets, U., and Reha-Krantz, L.J. (2005). Sensitivity to phosphonoacetic acid: a new phenotype to probe DNA polymerase delta in Saccharomyces cerevisiae. Genetics *170*, 569–580.

Lisby, M., Rothstein, R., and Mortensen, U.H. (2001). Rad52 forms DNA repair and recombination centers during S phase. Proc. Natl. Acad. Sci. USA *98*, 8276–8282.

Marsischky, G.T., and Kolodner, R.D. (1999). Biochemical characterization of the interaction between the Saccharomyces cerevisiae MSH2-MSH6 complex and mispaired bases in DNA. J. Biol. Chem. *274*, 26668–26682.

Marsischky, G.T., Filosi, N., Kane, M.F., and Kolodner, R. (1996). Redundancy of Saccharomyces cerevisiae MSH3 and MSH6 in MSH2-dependent mismatch repair. Genes Dev. *10*, 407–420.

Matic, I., Rayssiguier, C., and Radman, M. (1995). Interspecies gene exchange in bacteria: the role of SOS and mismatch repair systems in evolution of species. Cell *80*, 507–515.

Mendillo, M.L., Mazur, D.J., and Kolodner, R.D. (2005). Analysis of the interaction between the Saccharomyces cerevisiae MSH2-MSH6 and MLH1-PMS1 complexes with DNA using a reversible DNA end-blocking system. J. Biol. Chem. *280*, 22245–22257.

Morrison, A., Bell, J.B., Kunkel, T.A., and Sugino, A. (1991). Eukaryotic DNA polymerase amino acid sequence required for 3′----5′ exonuclease activity. Proc. Natl. Acad. Sci. USA *88*, 9473–9477.

Morrison, A., Johnson, A.L., Johnston, L.H., and Sugino, A. (1993). Pathway correcting DNA replication errors in Saccharomyces cerevisiae. EMBO J. *12*, 1467–1473.

Newport, J., and Yan, H. (1996). Organization of DNA into foci during replication. Curr. Opin. Cell Biol. *8*, 365–368.

Nick McElhinny, S.A., Stith, C.M., Burgers, P.M., and Kunkel, T.A. (2007). Inefficient proofreading and biased error rates during inaccurate DNA synthesis by a mutant derivative of Saccharomyces cerevisiae DNA polymerase delta. J. Biol. Chem. *282*, 2324–2332.

Nick McElhinny, S.A., Gordenin, D.A., Stith, C.M., Burgers, P.M., and Kunkel, T.A. (2008). Division of labor at the eukaryotic replication fork. Mol. Cell *30*, 137–144.

Park, J., Jeon, Y., In, D., Fishel, R., Ban, C., and Lee, J.B. (2010). Single-molecule analysis reveals the kinetics and physiological relevance of MutL-ssDNA binding. PLoS ONE *5*, e15496.

Peltomäki, P. (2003). Role of DNA mismatch repair defects in the pathogenesis of human cancer. J. Clin. Oncol. *21*, 1174–1179.

Pluciennik, A., Dzantiev, L., Iyer, R.R., Constantin, N., Kadyrov, F.A., and Modrich, P. (2010). PCNA function in the activation and strand direction of MutLα endonuclease in mismatch repair. Proc. Natl. Acad. Sci. USA *107*, 16066–16071.

Prolla, T.A., Pang, Q., Alani, E., Kolodner, R.D., and Liskay, R.M. (1994). MLH1, PMS1, and MSH2 interactions during the initiation of DNA mismatch repair in yeast. Science *265*, 1091–1093.

Pursell, Z.F., Isoz, I., Lundström, E.B., Johansson, E., and Kunkel, T.A. (2007). Yeast DNA polymerase epsilon participates in leading-strand DNA replication. Science *317*, 127–130.

Putnam, C.D., Hayes, T.K., and Kolodner, R.D. (2009). Specific pathways prevent duplication-mediated genome rearrangements. Nature *460*, 984–989.

Schmutte, C., Sadoff, M.M., Shim, K.S., Acharya, S., and Fishel, R. (2001). The interaction of DNA mismatch repair proteins with human exonuclease I. J. Biol. Chem. *276*, 33011–33018.

Shell, S.S., Putnam, C.D., and Kolodner, R.D. (2007). The N terminus of Saccharomyces cerevisiae Msh6 is an unstructured tether to PCNA. Mol. Cell *26*, 565–578.

Shibahara, K., and Stillman, B. (1999). Replication-dependent marking of DNA by PCNA facilitates CAF-1-coupled inheritance of chromatin. Cell *96*, 575–585.

Sia, E.A., Kokoska, R.J., Dominska, M., Greenwell, P., and Petes, T.D. (1997). Microsatellite instability in yeast: dependence on repeat unit size and DNA mismatch repair genes. Mol. Cell. Biol. *17*, 2851–2858.

Smith, B.T., Grossman, A.D., and Walker, G.C. (2001). Visualization of mismatch repair in bacterial cells. Mol. Cell *8*, 1197–1206.

Tishkoff, D.X., Boerger, A.L., Bertrand, P., Filosi, N., Gaida, G.M., Kane, M.F., and Kolodner, R.D. (1997). Identification and characterization of Saccharomyces cerevisiae EXO1, a gene encoding an exonuclease that interacts with MSH2. Proc. Natl. Acad. Sci. USA *94*, 7487–7492.

Tran, H.T., Gordenin, D.A., and Resnick, M.A. (1999). The 3′—>5′ exonucleases of DNA polymerases delta and epsilon and the 5′—>3′ exonuclease Exo1 have major roles in postreplication mutation avoidance in Saccharomyces cerevisiae. Mol. Cell. Biol. *19*, 2000–2007.

Tran, P.T., Simon, J.A., and Liskay, R.M. (2001). Interactions of Exo1p with components of MutLalpha in Saccharomyces cerevisiae. Proc. Natl. Acad. Sci. USA *98*, 9760–9765.

Umar, A., Buermeyer, A.B., Simon, J.A., Thomas, D.C., Clark, A.B., Liskay, R.M., and Kunkel, T.A. (1996). Requirement for PCNA in DNA mismatch repair at a step preceding DNA resynthesis. Cell *87*, 65–73.

Wang, H., and Hays, J.B. (2002). Mismatch repair in human nuclear extracts. Quantitative analyses of excision of nicked circular mismatched DNA substrates, constructed by a new technique employing synthetic oligonucleotides. J. Biol. Chem. *277*, 26136–26142.

Zanders, S., Ma, X., Roychoudhury, A., Hernandez, R.D., Demogines, A., Barker, B., Gu, Z., Bustamante, C.D., and Alani, E. (2010). Detection of heterozygous mutations in the genome of mismatch repair defective diploid yeast using a Bayesian approach. Genetics *186*, 493–503.

Zhang, Y., Yuan, F., Presnell, S.R., Tian, K., Gao, Y., Tomkinson, A.E., Gu, L., and Li, G.M. (2005). Reconstitution of 5′-directed human mismatch repair in a purified system. Cell *122*, 693–705.

Zou, H., and Rothstein, R. (1997). Holliday junctions accumulate in replication mutants via a RecA homolog-independent mechanism. Cell *90*, 87–96.